Preliminary Characterization of the Digitally Formed Beams of PHAROS2 Phased Array Feed

Giuseppe Pupillo[#], Alessandro Navarrini[*], Andrea Melis[*], Raimondo Concu[*], Pierluigi Ortu[*], Pasqualino Marongiu[*], Giovanni Naldi[#], Simone Rusticelli[#], Andrea Saba[$], Alessandro Scalambra[#], Luca Schirru[*], Adelaide Ladu[*], Tonino Pisanu[*], Enrico Urru[*]

[#]INAF-Institute of Radio Astronomy, Italy
[*]INAF-Astronomical Observatory of Cagliari, Italy
[$]ASI-Italian Space Agency, Italy

{giuseppe.pupillo, alessandro.navarrini, andrea.melis, raimondo.concu, pierluigi.ortu, pasqualino.marongiu}@inaf.it,
{giovanni.naldi, simone.rusticelli, andrea.saba, alessandro.scalambra}@inaf.it,
{luca.schirru, adelaide.ladu, tonino.pisanu, enrico.urru}@inaf.it, andrea.saba@asi.it

***Abstract* — We describe the beamforming strategy and the preliminary laboratory characterization results of the beam pattern synthesized by the PHAROS2 Phased Array Feed (PAF), a 4-8 GHz PAF with digital beamformer for radio astronomy application. The PAF is based on an array of 10×11 dual-polarization Vivaldi antennas cryogenically cooled at 20 K along with low noise amplification modules (LNAs) cascaded with a multi-channel Warm Section (WS) receiver. We present the beamforming and test procedures used to, respectively digitally synthesize and characterize the PHAROS2 antenna array beam pattern at 6 GHz. The tests of the array were carried out at room temperature by directly connecting 24 antenna elements to the WS and iTPM digital beamformer in a laboratory measurement setup.**

***Keywords* — Phased arrays, receiving antennas, radio astronomy, Vivaldi antennas, cryogenic electronics.**

I. INTRODUCTION

High-sensitivity large-scale surveys are an essential tool for discoveries in radio astronomy. A PAF placed at the focal plane of an antenna can increase the Field-of-View (FoV) and the mapping efficiency by fully sampling the sky [1]-[2]-[3]. A PAF consists of closely packed antenna elements with about half wavelength element separation that, by spatially sampling the focal plane, can synthesize multiple independent beams and be set to Nyquist-sample the sky. Multiple beams are formed by electronically adding the signals from different groups of radiating elements of the array. An antenna element can contribute to forming multiple beams. The properties of the beams can be optimized over a wide range of frequencies by electronically controlling each element phase and amplitude (complex weights) leading to high aperture efficiency and low spillover.

PHAROS (PHased Arrays for Reflector Observing Systems) [4]-[7] is a cryogenically cooled PAF demonstrator with an analogue beamformer based on an array of dual-polarization 10×11 Vivaldi antennas designed for radio astronomy observation across the 4-8 GHz band. The array, shown in Fig. 1, is cooled to 20 K along with 24 low noise amplifiers (LNAs) mounted directly behind the array elements.

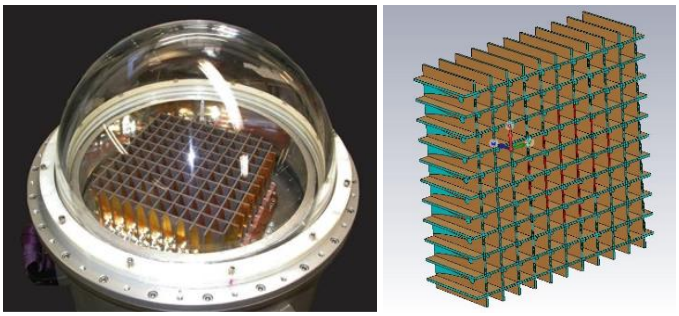

Fig. 1. Photo of PHAROS array of 10×11 Vivaldi dual polarization antennas and hemispherical vacuum window (left panel). Only the 24 central elements of the array vertical polarization (ports outlined in red on the 3D drawing on the right panel) are used for beamforming, the rest are matched terminated. PHAROS and PHAROS2 adopt the same antenna array. The array has a square shape with ≈230 mm side.

PHAROS2 [8], the upgrade of PHAROS, is a cryogenically cooled PAF with a digital beamformer for the 4-8 GHz band. The instrument is under development in the framework of the PAF SKA (Square Kilometer Array) [9] Advanced Instrumentation Program. PHAROS2 is a technology demonstrator resulting from the international collaboration of five European research institutes. A block diagram of the PHAROS2 PAF is illustrated in Fig. 2. The PAF features the following: *a)* a cryostat enclosing the PHAROS array of cryogenically cooled Vivaldi antennas, in which a sub-array of 24 antenna elements is cascaded with new generation LNAs with state-of-the-art performance (to reduce the system noise temperature); *b)* a 2.3-8.2 GHz room-temperature "Warm Section" (WS) multi-channel receiver [10]-[13]; and *c)* an FPGA-based Italian Tile Processing Module (iTPM) digital backend [14]-[15] capable of digitizing and synthesizing four independent beams across a ≈275 MHz IF band from a sub-array of 24 antenna elements. The IF signals are transported to the iTPM through WDM (Wavelength Division Multiplexing) IFoF (IF over fiber) technology. The WDM allows us to transport two IF signals over a single optical fiber. The main specifications of the PHAROS2 subsystems, including the array, the WS and the digital backend, are listed in Table 1. PHAROS2 is a PAF

demonstrator of a future high-sensitivity broadband PAF instrument that can find an application on single dish antennas like the Sardinia Radio Telescope [16].

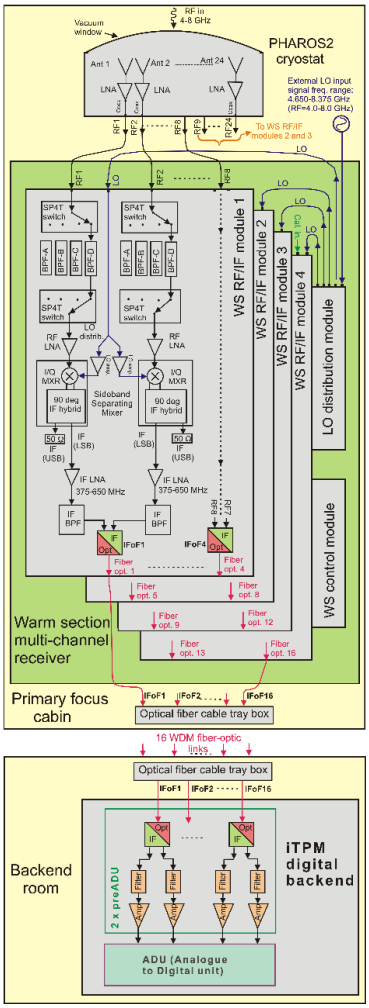

Fig. 2. Block diagram of the PAF receiver chain showing the PHAROS2 cryostat (top), the Warm Section multi-channel receiver (middle) and the iTPM digital backend (bottom). The schematic of the Warm Section multi-channel receiver, located in the primary focus receiver room, is enclosed by the green background rectangle.

II. Digital Acquisition and Frequency Channels

The iTPM Polyphase Filter Bank (PFB) acquires real samples (ADC sampling frequency f_s=700 MHz). It produces N=512 partially overlapped complex-valued frequency channels for each of the 24×IF 275 MHz-wide input signals from the sub-set of Vivaldi antenna array. The coarse channel separation is given by:

$$\Delta f = \frac{f_S}{2N} = \frac{700\ MHz}{1024} \approx 0.68\ MHz \qquad (1)$$

An overlapping factor of 32/27 determines a coarse channel width of 0.81 MHz, larger than the channel separation. According to the scheme showed in Fig. 3, the central frequency of a given coarse channel *i* is given by:

$$f_{0i} = \frac{350}{512} i = 0.68 \times i\ [MHz] \qquad (2)$$

where *i* is the channel index (from *i*=0 to 511).

Table 1. PHAROS2 Main Sub-Systems Specification

Vivaldi array	Total number of antenna elements	220
	Number of active antenna elements	24
	RF band	4.0-8.0 GHz
Warm receiver section	Number of RF channels	32 (four × eight-channel RF/IF modules). 24 used.
	RF band	2.3-8.2 GHz
	Frequency conversion scheme	Sideband Separating Mixer in LSB (USB terminated)
	LO band	2.950-8.575 GHz
	IF band	375-650 MHz
	Filter banks: Band Pass Filter (BPF) freq. range and LO frequency	*BPF-A*: 2.300-8.200 GHz;
		BPF-B: 4.775-5.050 GHz;
		BPF-C: 5.780-6.055 GHz;
		BPF-D: 6.445-6.720 GHz;
	Fiber optics Tx	WDM: 2 IFs on 1 fiber
iTPM Digital backend	Number of WDM fiber-optics Rx	16 on the 2 pre-ADU boards
	ADCs	16 × dual-ADCs AD9680, 1 GS/s, ENOB=10.8
	FPGAs	2 × Xilinx Kintex Ultrascale XCU40 20 nm
	Number of synthesized beams and instantaneous coverage	Four beams implemented in the iTPM FPGAs for 24 antenna elements with 275 MHz bandwidth
	N. of frequency channels and resolution	512 channels, 0.81 MHz/ch. (32/27 overlapping factor)

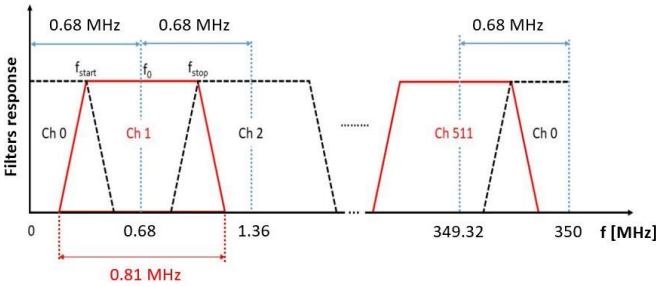

Fig. 3. Sketch of the overlapped coarse channels produced by the iTPM PFB.

III. Experimental Setup and Beam Characterization

A. Experimental setup

The digital beamforming capabilities of PHAROS2 were tested for the uncooled array (without cryostat, vacuum window, etc.) by directly connecting the outputs of 24 antennas to the WS receiver, without LNA, through 1 m long coaxial cables, as shown in Fig. 4. The measurements were made at ambient

temperature, which had no significant effect on the digital beamforming demonstration.

The array was located on a rotating platform that was revolved in azimuth by $\pm 90^0$ by steps of 2.5^0 around the vertical axis (see Fig. 5).

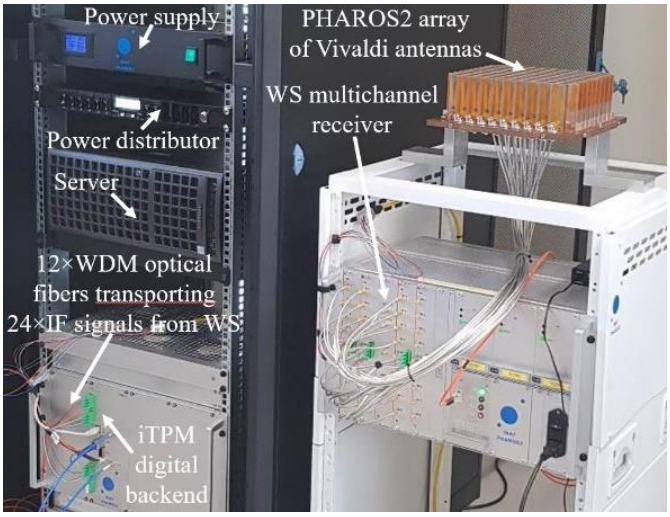

Fig. 4. Photo of PHAROS2 hardware used for analogue signal treatment (array of Vivaldi antennas, Warm Section multichannel receiver and pre-Analogue to Digital Unit) and digital beamforming by the iTPM backend, based on FPGAs.

The rotation axis was located on the phase centre of the array, placed on the aperture of the Vivaldi antennas. An RF transmitter, consisting of a double-ridged horn (Model A-9225-F from Officine Pasquali) connected to a signal generator (Rohde&Schwarz SMA110A) was aligned to the PHAROS2 array centre so that the 0^0 azimuthal angle identified the boresight direction. The separation between receiver and transmitter, of approximately d=3.8 m, was chosen to have the two antennas in the far-field of each other ($d>2D^2/\lambda$, where $D\approx$23 cm is the largest diameter of the PHAROS2 array and $\lambda\approx$5 cm). The test was carried out by transmitting a tone (10 dBm) at the RF frequency of ν_{RF}=6.0 GHz. The tone was downconverted by the PHAROS2 Warm Section receivers to the centre of the IF frequency band at ν_{IF}=512.5 MHz.

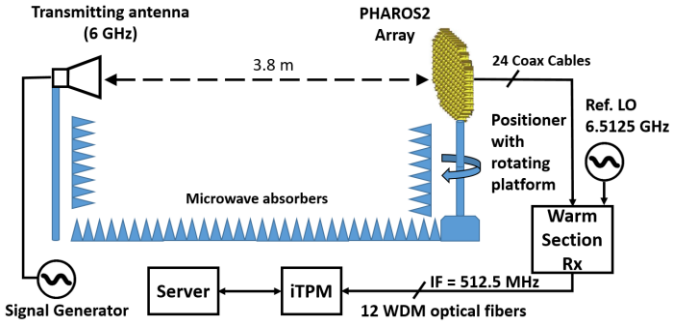

Fig. 5. Measurement setup for the PAF beamforming characterization. The array under test (right) sits on a platform that can be azimuthally rotated $\pm 90^0$ with respect to the direction identified by the RF transmitter (left).

It was received by the iTPM digital backend PFB frequency channel n. 275, by setting the Local Oscillator at ν_{LO}=6.5125 GHz. Microwave absorber panels were properly positioned in the test room to minimize the signal reflections and approximate the condition of an anechoic chamber.

B. *Test procedure*

One of the four PHAROS2 beams was digitally synthesized by a weighted combination of 24 active antenna elements. The main steps followed for the test procedure are summarized below.

a) The PHAROS2 array was pointed towards the transmitter boresight ($\theta = 0°$) and the iTPM was set in calibration mode. In this mode, the beamformer was disabled and the complex data voltages of all the 24 antennas, after the PFB channelizer, were acquired for about 90 s with a sampling rate of about 1.2 µsec. Two separate acquisitions were carried out: one with the Tx switched on and another one with the Tx switched off;

b) An off-line complex correlator software, we developed, calculated the output sample covariance matrix (ACM), as:

$$\boldsymbol{R} = \frac{1}{L}\sum_{n=1}^{L} \boldsymbol{x}(n)\boldsymbol{x}^H(n) \quad (3)$$

where $\boldsymbol{x}(n)$ is the n^{th} sample of the column vector of 24 complex voltages of each antenna element for a single 0.81 MHz coarse filter bank channel. The superscript H denotes the transpose conjugate of the complex vector and L the number of samples to be averaged. In our test $L = 2^{20}\approx 10^6$ samples, corresponding to an integration time of about 1.3 seconds;

c) From the ACMs, the beamformer weights for the boresight direction were calculated using the Conjugate Field Match (CFM) algorithm (see next subsection);

d) The beamformer weights were properly formatted and uploaded on the iTPM-FPGAs;

e) The PHAROS2 array was scanned in azimuth in the interval [-90°; +90°] from the boresight with 2.5° angular steps;

f) For each angle, the iTPM beamformer with calibrated weights provided directly the PAF antenna response with respect to the boresight.

C. *Calibration and beamforming algorithms*

In our tests, the beamformer weights were calculated using the CFM beamformer algorithm in which the weight vector for the direction Ω (here the boresight direction $\theta = 0°$) was estimated as follow:

$$\boldsymbol{w}_\Omega = \boldsymbol{u}_1 \quad (4)$$

where $\boldsymbol{u}_1$ is the dominant eigenvector of the matrix $\boldsymbol{R}_\Omega = \left(\boldsymbol{R}_\Omega^{on} - \boldsymbol{R}_\Omega^{off}\right)$. Since in a PAF the noise between antenna elements is usually strongly correlated, it is necessary to subtract the ACM obtained with the Tx switched off $\left(\boldsymbol{R}_\Omega^{off}\right)$ from that acquired when the Tx was radiating the signal $(\boldsymbol{R}_\Omega^{on})$ [17]. In general, the CFM beamformer does not maximize the sensitivity. The sensitivity, expressed in terms of

A_{eff}/T_{sys}, can be maximized when the weight vector is calculated by:

$$\boldsymbol{w}_{\Omega} = \left(\boldsymbol{R}_{\Omega}^{off}\right)^{-1}\boldsymbol{u}_1 \qquad (5)$$

Under the assumption of a point-like signal source and without interference, this method is equivalent to the classical max-SNR beamformer [17]. Our calibration software also implements this second algorithm (max-SNR), although this has not yet been tested on our experimental data.

D. Results

A snapshot of the $\boldsymbol{R}_{\Omega}^{on}$ and $\boldsymbol{R}_{\Omega}^{off}$ amplitudes calculated by (3) for the frequency channel #275 (6 GHz), at which the CW tone was transmitted, are illustrated in Fig. 6. These matrices were used in the calibration procedure described in Section C. Since they are acquired before the array calibration, the ACM amplitudes show the gain difference between the array elements. In particular, the antenna elements n. 16 and n. 19 exhibit a significantly lower gain than the other active elements.

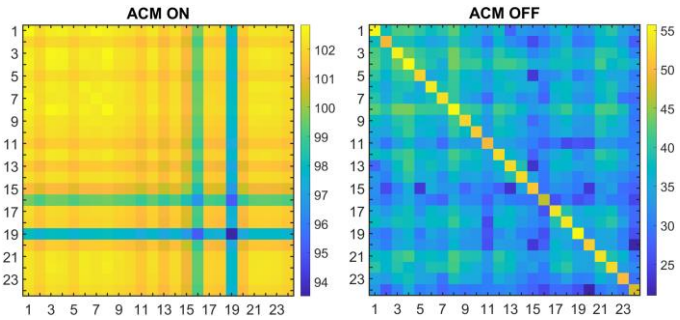

Fig. 6. Array Covariance Matrix amplitudes measured at the frequency channel # 275 when the transmitter was switched on (left) and off (right).

The preliminary measurement of the PHAROS2 H-plane power pattern at 6 GHz for the calibrated array beam is shown in Fig. 7. The black dots are the experimental data points, while the red curve is the cubic spline interpolation of the data.

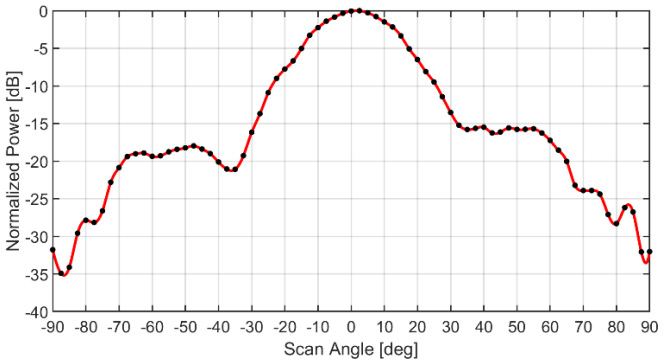

Fig. 7. Measured PHAROS2 beam pattern at 6 GHz formed by the iTPM digital back-end.

The measured full width half maximum (FWHM) of the array beam was of about 26.5°, in good agreement with the 26.0° value predicted by the electromagnetic simulations performed with the commercial software CST Microwave Studio. This is a preliminary result obtained in an experiment mainly aimed at testing and validation of the digital beamformer and the calibration algorithms. Full characterization and validation of the PHAROS2 beam pattern, through the comparison with the electromagnetic simulations, would require a more accurate measurement carried out within an anechoic chamber.

REFERENCES

[1] J.R. Fisher, R.F. Bradely, "Full-sampling array feeds for radio telescopes," Proceedings of SPIE Astronomical Telescopes and Instrumentation, Vol 4015, 2000.

[2] K. Warnick, R. Maaskant, M.V. Ivashina, D.B. Davidson, B.D. Jeffs, "High-Sensitivity Phased Array Receivers for Radio Astronomy, Proceedings of the IEEE, Vol. 104, Issue 3, pp. 607-622, March 2016.

[3] D. Anish Roshi et al., "Performance of a highly sensitive, 19-element, dual-polarization, cryogenic L-band phased array feed on the Green Bank Telescope," The Astronomical Journal, 155:202, May 2018.

[4] J. Simons, M. Ivashina, J. G. b. d. Vaate, and N. Roddis, "Beamformer system model of focal plane arrays in deep dish radio telescopes," European Radar Conf. EURAD 2005, Paris, France, 3-4 October 2005.

[5] J. Simons, J.G. Bij de Vaate, M.V. Ivashina, M. Zuliani, V. Natale, N. Roddis, "Design of a focal plane array system at cryogenic temperatures," Proc. 'EuCAP 2006', Nice, France, 6–10 Nov. 2006.

[6] W. Ciccognani, F. Di Paolo, F. Giannini, E. Limiti, P.E. Longhi, A. Serino, "A GaAs Front-end Receiver for Radio Astronomy Applications," 13th IEEE Melecon 2006, May 16-19, Spain.

[7] L. Liu, K. Grainge, and A. Navarrini, "Analysis of Vivaldi array antenna for phased array feeds application," IEEE MTT-S Int. Conf. on Num. Elec. and Multiph. Mod. and Opt. for RF, Micr., and THz App. (NEMO), Seville, Spain, 17-19 May, 2017.

[8] A. Navarrini et al., "Design of PHAROS2 Phased Array Feed," Proc. of 2nd URSI Atl. Radio Sci. Meet. (AT-RASC), Gran Canaria, Spain, 28 May – 1 June 2018.

[9] A. van Ardenne, J.D. Bregman, W.A. van Cappellen, G.W. Kant, J.G. Bij de Vaate, "Extending the Field of View with Phased Array Techniques: Results of European SKA Research." Proc. IEEE 2009, 97, 1531–1542.

[10] A. Navarrini, A. Scalambra, S. Rusticelli, A. Maccaferri, A. Cattani, F. Perini, P. Ortu, J. Roda, P. Marongiu, A. Saba, M. Poloni, A. Ladu, L. Schirru, "The Room Temperature Multi-Channel Heterodyne Receiver Section of the PHAROS2 Phased Array Feed" MDPI Electronics, Vol. 8, Issue 6, 666, June 2019.

[11] A. Navarrini, A. Scalambra, S. Rusticelli, A. Maccaferri, A. Cattani, F. Perini, P. Ortu, J. Roda, P. Marongiu, A. Saba, M. Poloni, A. Ladu, "A 2.3-8.2 GHz Room Temperature Multi-Channel Receiver for Phased Array Feed Application." Proc. of IEEE UKRCON Conference, Lviv, Ukraine, July 2-6, 2019, DOI: 10.1109/UKRCON.2019.8879848.

[12] A. Navarrini et al., "The Warm Receiver Section and the Digital Backend of the PHAROS2 Phased Array Feed," IEEE International Symposium on Phased Array Systems and Technology, Waltham, MA, USA, Oct. 15-18, 2019.

[13] P. Ortu, A. Saba, P. Marongiu, F. Gaudiomonte, A. Navarrini, A. Cattani, A. Maccaferri, A.Scalambra, "Control Box of PHAROS2", INAF Technical Report n. 4, 2020-01-10T10:28:22Z, Available at: https://openaccess.inaf.it/handle/20.500.12386/23053.

[14] G. Naldi et al., "Development of a new digital signal processing platform for the Square Kilometer Array." Proc. of 2nd URSI Atl. Radio Sci. Meet. (AT-RASC), Gran Canaria, Spain, 28 May – 1 June 2018.

[15] G. Comoretto, et al. "The Signal Processing Firmware for the Low-Frequency Aperture Array." Journal of Astronomical Instrumentation, Vol. 6, n. 1, 201, 2017.

[16] A. Navarrini et al., "Electromagnetic simulation and beam-pattern optimization of a C-band Phased Array Feed for the Sardinia Radio Telescope." Proc. of IEEE UKRCON Conference, Lviv, Ukraine, July 2-6, 2019, DOI: 10.1109/UKRCON.2019.8879888.

B.D. Jeffs, K.F. Warnick, J. Landon, J. Waldron, D. Jones, J.R. Fisher, R.D. Norrod "Signal Processing for Phased Array Feeds in Radio Astronomical Telescopes", IEEE Journal of Selected Topics in Signal Processing, Vol. 2, No. 5, October 2008.